A comprehensive evaluation of murine and human *ex vivo* cultured alveolar macrophages

Camille David[1,2], Deborah Brea[1,2], Charles Verney[1,2,3], Adeline Cezard[1], Virginie Vasseur[1], Benoit Briard[1], Sandra Khau[1], Emilie Barsac[1,2], Marion Ferreira[1,4], Sylvain Marchand-Adam[1,4], Mustapha Si-Tahar[1,2] and Antoine Guillon[1,2,3]

[1]INSERM, Centre d'Etude des Pathologies Respiratoires, UMR 1100, Tours, France. [2]Université de Tours, Tours, France. [3]CHRU de Tours, Service de Médecine Intensive Réanimation, Tours, France. [4]CHRU de Tours, Service de Pneumologie et Explorations Fonctionnelles Respiratoires, Tours, France.

Antoine Guillon (antoine.guillon@univ-tours.fr)

Shareable abstract (@ERSpublications)
Isolated alveolar macrophages (AMs) from mice and humans can be cultured for several days (humans) or months (mice). Mouse and human AMs share functions but present some differences in magnitude of TLR responses and regarding programmed cell death. https://bit.ly/3C92nMC

Cite this article as: David C, Brea D, Verney C, *et al*. A comprehensive evaluation of murine and human *ex vivo* cultured alveolar macrophages. *ERJ Open Res* 2025; 11: 00859-2024 [DOI: 10.1183/23120541.00859-2024].

Received: 26 Aug 2024
Accepted: 27 Oct 2024

Abstract

Background Alveolar macrophages (AMs) serve as the frontline defence in the lungs; however, comprehensive cell culture models for their study remain limited. Freshly isolated AMs are hindered by restricted quantities (mice) or challenges in accessing donors (humans). Recently, murine fetal liver-derived macrophages cultured with granulocyte–macrophages colony-stimulating factor were proposed as AMs-like macrophage (called MPI). Furthermore, recent technical progress improved the culture and expansion of primary murine AMs.

Methods We examined three distinct *in vitro* models of alveolar macrophages: MPI, long-term culture-expanded AMs from mice (mAM) and cultured from human (hAM), aiming to compare and elucidate their respective advantages.

Results We observed that: 1) isolated AMs from mice and humans can be cultured for several days (human) or months (mice) with minor loss of AM-specific surface markers expression over time; 2) MPI is a self-replicative macrophage model that is easy to culture but lacks the typical AM surface expression marker (*i.e.* SiglecF) and presents a constitutive pro-inflammatory phenotype; 3) responses to Toll-like receptor (TLR) agonists are consistent between MPI, mAM and hAM models but differences in magnitude should be considered; 4) phagocytic activity of MPI, mAM and hAM were similar; 5) major differences were observed between murine and human AMs regarding programmed cell death, especially for MPI; and 6) ecological and ethical consequences of these AM models are different and sometimes opposed and should be carefully assessed.

Conclusion Our study provides a comprehensive comparison of *ex vivo* murine and human AM models and gives insight into the translational value of these different AM models.

Introduction

Alveolar macrophages (AMs) are crucial cells in lung immunity and homeostasis, comprising 80% of cells in human bronchoalveolar lavage fluid (BALF) and 95% of cells in mouse BALF [1, 2]. They continuously phagocytose inhaled pathogens, balancing rapid defence with minimal inflammation to maintain gas exchange [3].

Despite their importance, studying AMs is challenging due to limited culture models. While macrophages derived from murine bone marrow or human monocytes are widely used [4], they lack the tissue-specific characteristics of AMs. Additionally, *in vitro* models have faced criticism, particularly the oversimplified M1/M2 macrophage classification, which fails to capture the complexity of macrophage plasticity *in vivo* [5, 6].

New *in vitro* models aim to better mimic AMs. For instance, murine fetal liver-derived macrophages cultured with granulocyte–macrophages colony-stimulating factor (GM-CSF) produce "Max Planck Institute cells" (MPI), which are non-transformed and self-renewing [7]. However, MPI cells do not fully replicate AMs' characteristics as they do not account for monocyte-derived cell contributions and lack the lung environment that shapes AM identity [8]. Freshly isolated AMs offer a more accurate model but are limited by the difficulty of harvesting sufficient quantities. Recent advances have enabled the culture and expansion of murine AMs using weekly GM-CSF treatment [9, 10], though these still fail to capture the full heterogeneity of AM populations, which are constantly influenced by environmental factors over an organism's lifespan [3, 11]. This diversity, shaped by factors such as microbial exposure or inflammation, complicates the extrapolation of murine AM studies to humans.

To address these gaps, we propose a comparison of *ex vivo* murine AM and human AM culture models to evaluate their translational value. We studied three models: MPI cells, long-term culture-expanded murine AMs and cultured human AMs. We compared the evolution of AM-specific surface markers, inflammatory responses, phagocytic activity and programmed cell death kinetics. Additionally, we considered the economic, ecological and ethical aspects of these models to provide a comprehensive evaluation of their relevance for studying AM physiopathology.

Materials and methods

Mice

C57Bl/6 male and female mice were purchased from the Centre d'Elevage R. Janvier (Le Genest Saint-Isle, France) and were used at about 8–10 weeks of age. Mice were treated in accordance with the European animal welfare regulation. Mice were bred in an animal facility in pathogen-free conditions. All animal experimentations were performed according to the ethical guidelines and were approved by our local and national ethics committee (CEEA.19, #201604071220401-4885).

Human samples

Study of human samples was approved by the institutional review board of the Tours University Hospital (Espace de Réflexion Éthique de la Région Centre), and the human sample collection was reported to the competent authority (Ministère Français de l'Enseignement Supérieur, de la Recherche et de l'Innovation, DC-2014-2285). Informed consent was obtained from all subjects. The study conformed to the principles set out in the Declaration of Helsinki and the Department of Health and Human Service Belmont Report.

Bronchoalveolar lavage (BAL) was performed in a pulmonology unit (CHRU of Tours, France) to isolate human AMs or to use directly for flow analysis. The exclusion criteria included active pulmonary infections, suspected or confirmed, based on the presence of: 1) symptoms such as cough, sputum production, fever, dyspnoea and chest pain; 2) elevated inflammatory biomarkers, including CRP and PCT, or an elevated neutrophil count; and 3) an abnormal chest radiograph showing lung consolidation. The main clinical and pathological characteristics of cohorts are summarised in table 1. The enrolled subjects were selected for their AM enrichment; around 87.5% (median value) of the cells were AMs as indicated in the table.

TABLE 1 Patients' characteristics (n=20) and bronchoalveolar lavage (BAL) cellularity

Sex, male	13 (59.1)
Age, years	67.5 (56.8–75)
Body weight, kg	75 (61.4–87.5)
Body mass index, kg·m^{-2}	27.2 (23.1–29.2)
Active smokers	3 (13.6)
Former smokers	6 (27.3)
Underlying lung disease	2 (9.1)
COPD	2 (9.1)
BALF cellularity	
Total cell count (per mm^3)	237 (152–478)
Alveolar macrophages, %	87.5
Lymphocytes, %	5.5
Polymorphonuclear neutrophils, %	2.2
Eosinophils, %	<1
Mast cells, %	<1
Microorganisms	0

Quantitative data are reported as median (IQR), qualitative value reported as n (%). BALF: bronchoalveolar lavage fluid.

MPI cell culture

A seed stock of MPI cells, generously given by Dr Francois Trottein (Pasteur Institute, Lille, France), and established and characterised at an earlier date [7], was used to generate all the MPI cells for this study. Cells were cultivated in a 10-cm Petri dish (cat. no. 633181, Griener) with RPMI 1640 medium (cat. no. 61870-010, Gibco) containing 10% fetal bovine serum (FBS), 100 $U \cdot mL^{-1}$ penicillin and 100 $\mu g \cdot mL^{-1}$ streptomycin (cat. no. P06-07100, PAN Biotech) and 15 $ng \cdot mL^{-1}$ of recombinant murine GM-CSF (cat. no. 315-03, PeproTech). MPI cells were further amplified and passaged twice a week at a concentration of 2×10^5 $cells \cdot mL^{-1}$ (2×10^6 cells/10 mL in a 10-cm Petri dish). MPI cells were detached using a cell-scrapper, centrifuged at 500 g for 10 min, counted and seeded at the indicated concentration. Cells from passages 11 to 40 were used.

Murine AMs

Fresh mBALF from female and male mice were used for flow analysis. It was performed using sterile saline buffer (at room temperature) consisting of four lavages of 0.5 mL. Retrieved cells were centrifuged. Red blood cells were lysed using the Red Blood Cell Lysing Buffer Hybri-Max (cat. no. R7757-100ML, Sigma-Aldrich) for 3 min. After a centrifugation step, cells were incubated in buffer described later for flow analysis in order to identify AMs.

For *ex vivo* culture, murine AMs (mAM) were cultured as previously described [2, 9]. Briefly, BALF from a pool of three to five mice was used. Red blood cells were lysed for 5 min and 2×10^6 cells were cultured in a 10-cm Petri dish with RPMI 1640 medium containing 10% FBS, 100 $U \cdot mL^{-1}$ penicillin, 100 $\mu g \cdot mL^{-1}$ streptomycin, 15 $ng \cdot mL^{-1}$ of recombinant murine GM-CSF and 1X solution of sodium pyruvate. After 3–4 h, non-adherent cells were washed three times with phosphate buffered saline (PBS) and fresh medium was added. Medium was changed every 2–3 days to maintain the culture, and cells were passaged when 70–90% confluency was reached. For this, cells were detached with Accutase (cat. no. 25-058-CI, Corning Inc.) containing 1 mM EDTA at 37°C for 30 min, centrifuged at 500 g for 10 min, counted and seeded at the indicated concentration. All the experiments were performed with mAM between passage 1 and 7 (at a rate of one passage every 3 weeks).

Human AMs

Fresh BALF was recovered at the pulmonology unit and maintained in ice. BAL was performed as previously described [12–14]. Samples were filtered under sterile condition (100 µm filter). Cells were centrifuged at 300 g for 10 min at 10°C. The pellet was washed with 2 mL of RPMI 1640 containing 2% FBS, 100 $U \cdot mL^{-1}$ penicillin, 100 $\mu g \cdot mL^{-1}$ streptomycin and 1.75 $ng \cdot mL^{-1}$ Amphotericin B (cat. no. A9528-50MG, Sigma-Aldrich) and centrifugated. Red blood cells were lysed for 5 min. Cells were treated as described above for flow analysis to identify AMs.

For *ex vivo* human AMs (hAM) culture, BALF was centrifuged, cells were counted and plated in a 10-cm or 20-cm (depending on the number of cells) Petri dish with RPMI 1640 medium containing 10% of FBS, 100 $U \cdot mL^{-1}$ penicillin, 100 $\mu g \cdot mL^{-1}$ streptomycin, 15 $ng \cdot mL^{-1}$ of recombinant human GM-CSF (cat. no. 300-03, PeproTech), 1% non-essential amino acids (cat. no. 11140-035, Gibco), 10 mM HEPES and 100 $\mu g \cdot mL^{-1}$ primocin (cat. no. ant-pm-1, InvivoGen). After 3–4 h, non-adherent cells were washed three times with PBS and the same medium was added until experiments the next day for fresh hAM. For cultured hAM, medium was changed every 2–3 days to maintain the culture until the experiments. Cells were detached and seeded as mAM.

May–Grünwald Giemsa staining

MPI, mAM, hAM and BALF were spun at a concentration of 5–7.5×10^4 cells/0.4 mL on an EZ Single Cytofunnel (cat. no. A78710020, Epredia) for 10 min at 300 rpm using a Cytospin 4 (Thermo Scientific), and subsequent May–Grünwald Giemsa staining was used following the manufacturer's (cat. no. RAL-3200700500, Fisher Scientific) instructions.

Flow cytometry

Cell suspensions of MPI, mAM, hAM and BALF were incubated in PBS containing 2% FCS, 2 mM EDTA and 5% home-made anti-CD16/32 (2.4G2) (FACS buffer) for 20 min at 4°C. Cells were stained with LIVE/DEAD Fixable Aqua Dead Cell Stain Kit (cat. no. L34966, Thermo Fisher Scientific; 1/1000 dilution), and a combination of monoclonal antibodies for 30 min on ice in the dark, and then washed with FACS buffer. Antibodies used are listed in supplementary table S1. Flow cytometry data were acquired on a MACSQuant Analyzer (Milteny Biotech), and data were analysed with FlowJo software (v10.4.2).

Cells stimulation

All cell types were seeded in 96-well plates (2.105 cells/200 µL) in their respective medium the day before the experiment without GM-CSF for each cell type. Cells were stimulated (2.105 cells/100 µl) with 4 $mg \cdot mL^{-1}$ of disodium succinate (cat. no. W327700, Sigma-Aldrich), 20 $\mu g \cdot mL^{-1}$ of Poly (I: C) (cat. no. tlr-pic, InvivoGen), 0.1 $\mu g \cdot mL^{-1}$ of lipopolysaccharide (LPS) (cat. no. tlr-pb5lps, InvivoGen), 0.4 $\mu g \cdot mL^{-1}$ of recombinant flagellin, 1 $\mu g \cdot mL^{-1}$ of Pam3CSK4 (cat. no. tlrl-pms, InvivoGen) or 20 $\mu g \cdot mL^{-1}$ curdlan (cat. no. tlrl-curd, InvivoGen) in RPMI 1640 medium containing 10% of FBS. Supernatants were collected after 6 h of stimulation for all the agonists and 24 h in addition for disodium succinate stimulation.

Real-time cell death analysis

Real-time cell death assays were performed using a two-colour IncuCyte SX5 cell-live analysis system (Sartorius). All cell types were seeded and stimulated as described above in medium containing 1 µM of the DNA-binding fluorescent dye propidium iodide (PI) (cat. no. P4170-25MG, Sigma-Aldrich). Cells were stimulated with 100 $ng \cdot mL^{-1}$ of LPS (cat. no. L3024-5MG, Sigma-Aldrich) for 4 h, and 5 mM of ATP (cat. no. tlrl-atpl, InvivoGen) was added before scanning (LPS+ATP condition) or 20 µM of the inhibitor of apoptosis protein inhibitor BV6. Supernatants were collected for quantification of cytokines after 6 or 24 h of stimulation. For real-time analysis, experiments were conducted using four to nine image fields per well during 24 h, and resulting images were analysed using the software package supplied with the IncuCyte imager, which allows determination of the dead cell events *via* red PI positive objects (cell nucleus), and plotted using Prism software (GraphPad Prism 8.0.2).

Phagocytosis assay

All cell types were seeded in 96-well plates (1–2.10^5 cells/100 µL) in their respective medium the day before the experiment. Incucyte pHrodo Red Zymosan Bioparticles (cat. no. 4617, Essen Bioscience) were used to evaluate the phagocytosis capacity of each cell type using a two-colour IncuCyte SX5 cell-live analysis system permitting a dynamic and real-time lapse manner. Briefly, 5 µg of zymosan in RPMI 1640 medium containing 10% of FBS were added to the plate. Cytochalasin D (CytoD) (cat. no. C8273-1MG, Sigma-Aldrich), which inhibits the phagocytosis, is used as control. For this condition, 1 $\mu g \cdot mL^{-1}$ of CytoD was added prior to the addition of zymosan. Automated imaging and quantification analysis were performed for 6 h. Experiments were conducted as described above except for the quantification of cells containing red zymosan bioparticles. After 6 h, cells were detached and processed for flow cytometric analysis.

ELISA

Duoset ELISA (mouse and human tumour necrosis factor-α (TNF-α), interleukin (IL)-6, IL-1β) was performed according to the manufacturer's instructions (R&D Systems).

Economic and ecological costs

To quantify the potential ecological impacts of the experimental model set-up, we assessed the weight of all plastic used (converted into CO_2 emission required for plastic production) and the energy consumed by a 165-L volume capacity-cell incubator (New Brunswick Galaxy 170S, Eppendorf), being 0.1 kWh to maintain the 37°C temperature of culture. At the end, we were able to determine the weight of plastic used, time of incubation, energy needed, CO_2 emissions and economic costs for all three models (table 2).

Statistical analysis

Data were plotted using Prism software (GraphPad Prism 8.0.2).

TABLE 2 Ecological and economics costs to generate 6×10^6 cells of MPI, mAM and hAM culture

	MPI	mAM	hAM
Total weight of plastic used, g	41.7	239.3	115.8
Time of incubation, days	3	21	10
Energy needed, kWh	9.6	67.5	32.1
Total CO_2 emission, kg	8.5	60.4	28.6
Total economic cost, euros	13.4	103.1	50.8

MPI: "Max Planck Institute cells"; mMAM: murine alveolar macrophages; hAM: human alveolar macrophages.

Results

Phenotype and evolution of lineage-specific surface markers of murine and human AMs models in culture

Utilising primary cultures of AMs has the potential to enhance our understanding of AM biology, but it is crucial to acknowledge that experimental conditions may modify the typical AM phenotype. To address this, we cultured MPI cells as previously described [7] and obtained mAM from mBALF using a simple and straightforward procedure. Consistent with recent observations [9], mAM could be kept in continuous culture for several months.

We compared cellular morphologies of MPI and 4-month cultured mAM, with freshly collected mBALF of a naive mouse (considered as the gold standard). Both MPI and mAM displayed a typical AM phenotypic appearance as assessed by May–Grünwald Giemsa (MGG) coloration (figure 1a) and forward scatter (FSC) and side scatter (SSC) profile (supplementary figure S1a). In our culture conditions, MPI were $CD45^{+}CD64^{+}CD11b^{+}CD11c^{+/-}$ but showed no SiglecF surface expression (figure 1b and supplementary figure S1a). For mAM, after 6 months of *ex vivo* culture, the phenotype $CD45^{+}SiglecF^{+}CD11c^{+}CD64^{+}$ was conserved with a slight decrease for CD11c compared to AMs gated from a fresh mBALF (figure 1b and supplementary figure S1b). We examined CD11c and SiglecF expressions of mAM at different time points during the expansion. We observed minor decreases that seemed to be inversely correlated with the number of cell passages especially for CD11c with a minor decrease for SiglecF, but mAM still conserved their lineage-specific surface markers, even after a freezing/thawing cycle (supplementary figure S1b). Despite these minor modifications, our results show a clear potential of mAM for expansion and *ex vivo* culture for months.

Next, we assessed whether AMs from human BALF (hBALF) could be cultured for several days. The patients' characteristics are presented in table 1. We collected fresh hBALF and performed direct flow cytometric analysis and isolation/culture of hAM. Flow cytometry strategy was based as previously described [15]. After 10 days of maintenance, cultured hAM presented the same morphology as cells from fresh hBALF (figure 1c). Cultured hAM well-maintained the $CD45^{+}HLA\text{-}DR^{+}CD11b^{+}CD169^{+}CD206^{+}CD15^{-}$ phenotype without alterations in surface marker expressions compared to hAM gated from the fresh hBALF (figure 1d, e and supplementary figure S1c). We did not observe expansion of hAM. Overall, isolated AMs could be cultured for days (hAM) and months (mAM) conserving their AM features, whereas MPI presented almost all the AM-like features except for SiglecF expression.

MPI, mAM and hAM present different inflammatory signatures in response to pro-inflammatory agonists

When stimulated, AMs initiate inflammation by producing various chemokines and cytokines [3]. We selected TNF-α, IL-6 and IL-1β as critical cytokines in host immunity, to monitor the production of inflammatory mediators by MPI, mAM and hAM. These cells were exposed to different Toll-like receptor (TLR) agonists: bacterial LPS (TLR4 agonist), polyinosinic-polycytidylic acid (poly(I:C), TLR3 agonist), flagellin (Flag, TLR5 agonist), Pam3CysSerLys4 (Pam3CSK4, TLR2/1 agonist) and Curdlan (TRL2/TLR6 agonist).

Firstly, we compared the immune response of freshly isolated AMs from three human donors by BALF (referred to as fresh hAM) with hAM cultured up to 10 days for the same donors (figure 2a). With few exceptions, cultured hAM showed similar trends of cytokine production compared to fresh hAM in response to various TLR agonists (figure 2a). Working with hAM immediately after the BAL procedure is challenging on a daily basis due to the unpredictability of sampling, which makes it difficult to plan and execute complex experiments. Therefore, we preferred to work with hAM that had been cultured for a few days. In the absence of cell expansion, we see no advantage to perform freeze–thaw cycles.

We next deciphered the immune response of MPI, cultured mAM and cultured hAM. For all the cultured models, the overall pattern of inflammatory mediator production was similar between MPI and mAM when exposed to a wide range of TLR agonists (figure 2b–e) with notable differences observed in the magnitude of the response. MPI secreted more pro-inflammatory cytokines compared to mAM, as illustrated by a 4.6-, 4.7- and 2.2-fold increase in TNF-α, IL-6 and IL-1β, respectively, in response to LPS compared to mAM. Regarding human cells, hAM produced inflammatory mediators in response to poly(I:C), LPS and Pam3CSK4 exposure but at lower concentrations, particularly for TNF-α and IL-6 (figure 2a–c). Finally, no difference in the kinetic of IL-6 production was observed between mAM models and hAM (figure 2d). All AM models responded rapidly with a first significant increase at 4 h post challenge and a plateau thereafter (figure 2d). Overall, AMs of murine origin (MPI and mAM) demonstrated a more pro-inflammatory phenotype compared to hAM for certain stimuli.

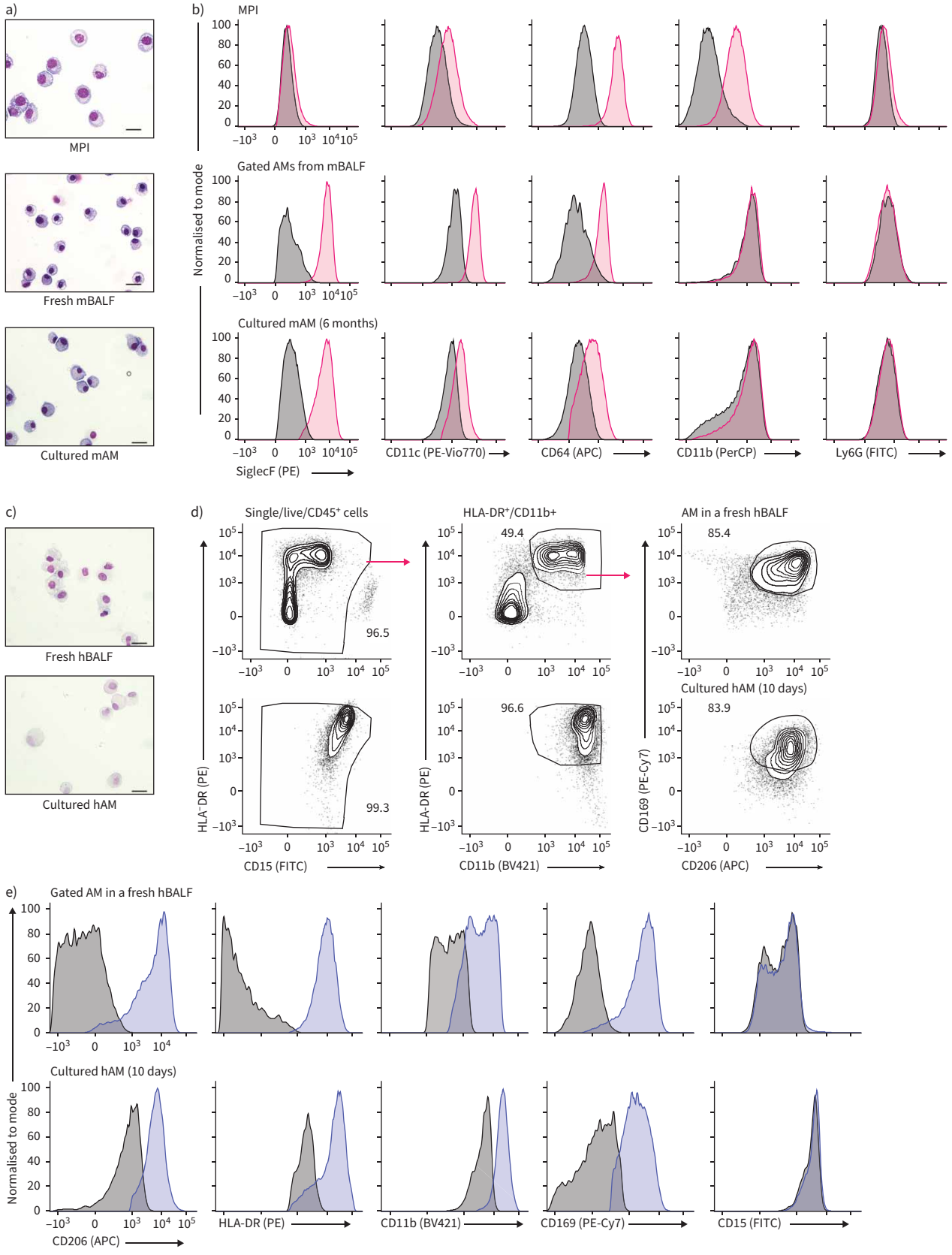

FIGURE 1 Phenotype evolution of murine and human alveolar macrophage models in culture. a) Representative pictures of MPI ("Max Planck Institute cells"), cells in fresh murine bronchoalveolar lavage fluid (mBALF) from a naive mouse and murine alveolar macrophages (mAM) cultured

for 4 months stained with May–Grünwald Giemsa. Scale bars: 25 µm. b) Expression of surface markers across single/live/CD45$^+$ MPI, gated AMs in a fresh mBALF from a naive mouse and mAM cultured for 6 months depicted as representative pink histogram. Grey histogram represents matched fluorescence −1 negative control. c) Representative pictures of cells collected in a fresh hBALF from human 3–4 h after the flexible bronchoscopy procedure (upper picture) and cultured human AM (hAM) (Day 10, lower picture). May–Grünwald Giemsa staining. Scale bars: 25 µm. d) Representative flow cytometry dot plots showing CD206, HLA-DR, CD11b, CD169 and CD15 expression in single/live/CD45$^+$ gated AMs in fresh hBALF and its isolated hAM after 10 days of culture. e) Expression of surface markers across gated AMs in a fresh hBALF and its isolated hAM after 10 days of culture depicted as a blue histogram. Grey histogram represents matched fluorescence −1 negative control. In parts a and b pictures are representative of two experiments (MPI and mAM) and three mBALF. In part c pictures represent one donor for fresh hBALF and cultured hAM, two technical replicates. In part d data are representative of two human donors for fresh hBALF and cultured hAM.

Recent findings suggest that mitochondrial-derived metabolites, known as metabokines, play signalling roles in immunity [16–20]. Succinate, an emerging metabokine derived from the tricarboxylic acid cycle, has received attention for its regulatory role in macrophage inflammation [20–22]. We assessed the production of inflammatory mediators in MPI, mAM and hAM exposed or not to succinate. hAM exposed to succinate did not express inflammatory cytokines at both early (6 h) and later (24 h) time points (supplementary figure S2a, b). In contrast, succinate induced a significant production of IL-6 and IL-1β in long-term cultured murine AMs, and to a lesser extent in MPI (supplementary figure S2a, b).

In summary, hAM and mAM models exhibit the same pattern in response to inflammatory triggers but with important and significant differences in amplitude.

Comparative functional analysis of MPI, mAM and hAM phagocytosis

Functional analysis of macrophages throughout phagocytosis offers crucial insights into their pivotal role in maintaining lung homeostasis. To compare the phagocytic activity of MPI, mAM and hAM, we tracked the dynamic uptake of fluorescent zymosan particles (pHrodo Red Zymosan BioParticles conjugate) with a cell-live analysis system (IncuCyte). Zymosan particles are derived from the cell walls of yeast. pHrodo Red dye conjugates are not fluorescent outside the cell but fluoresce bright red within phagosomes, specifically detecting intracellular phagocytosis. All AM models rapidly engulfed zymosan particles and emitted a fluorescent signal assessed by real-time monitoring (figure 3a, b). The phagocytic kinetics were rapid for all tested AM models: 71, 97 and 132 events·min^{-1} during the first hour for MPI, hAM and mAM, respectively, demonstrating no significant difference between mAM and hAM in the first hours but a lesser phagocytic speed for MPI (figure 3a, b). To further quantify the phagocytic rates, cytometric quantification was performed at 6 h post-zymosan incubation (figure 3c, d). Finally, we compared the phagocytic rates of hAM freshly isolated and then cultured for 10 days in two human donors and did not observed any differences (figure 3e).

Overall, the phagocytic activities of MPI, mAM and hAM were comparable, highlighting their shared efficiency in engulfing microbial particles.

Responses to programmed cell death triggers reveal important interspecies differences among AM models

Studying apoptosis and pyroptosis in macrophages is interesting due to their pivotal roles in immunity and tissue homeostasis. Apoptosis regulates immune responses by eliminating infected or damaged cells without causing excessive inflammation [23], whereas pyroptosis serves as an inflammatory defence mechanism, aiding in the elimination of pathogens while activating immune responses [24]. Here, we aimed to understand the similarities and differences between MPI, mAM and hAM regarding these two programmed cell death mechanisms.

We used LPS/ATP and BV6 as inducers of cell death [25, 26]. Our observations indicate significant differences in kinetics and sensitivities to cell death pathways among the AM models (figure 4). First, MPI and mAM showed an immediate and important pyroptosis upon LPS/ATP treatment, while hAM response was postponed and less extensive (figure 4a). Second, mAM and hAM presented similarities in response to BV6 that differ drastically from MPI (figure 4a).

To gain further insights into the inflammatory signalling triggered by cell death in the three AM models, we monitored the production of IL-1β and TNF-α. In hAM, apoptosis occurred without inducing inflammation (no IL-1β or TNF-α production whatever the time point). This result was not entirely recapitulated in mAM or MPI models as IL-1β production was observed, especially at late time points (figure 4b, c). Pyroptosis resulted in IL-1β production in all tested AM models. However, significant differences in the magnitude of inflammatory responses were noted, with MPI being drastically more responsive.

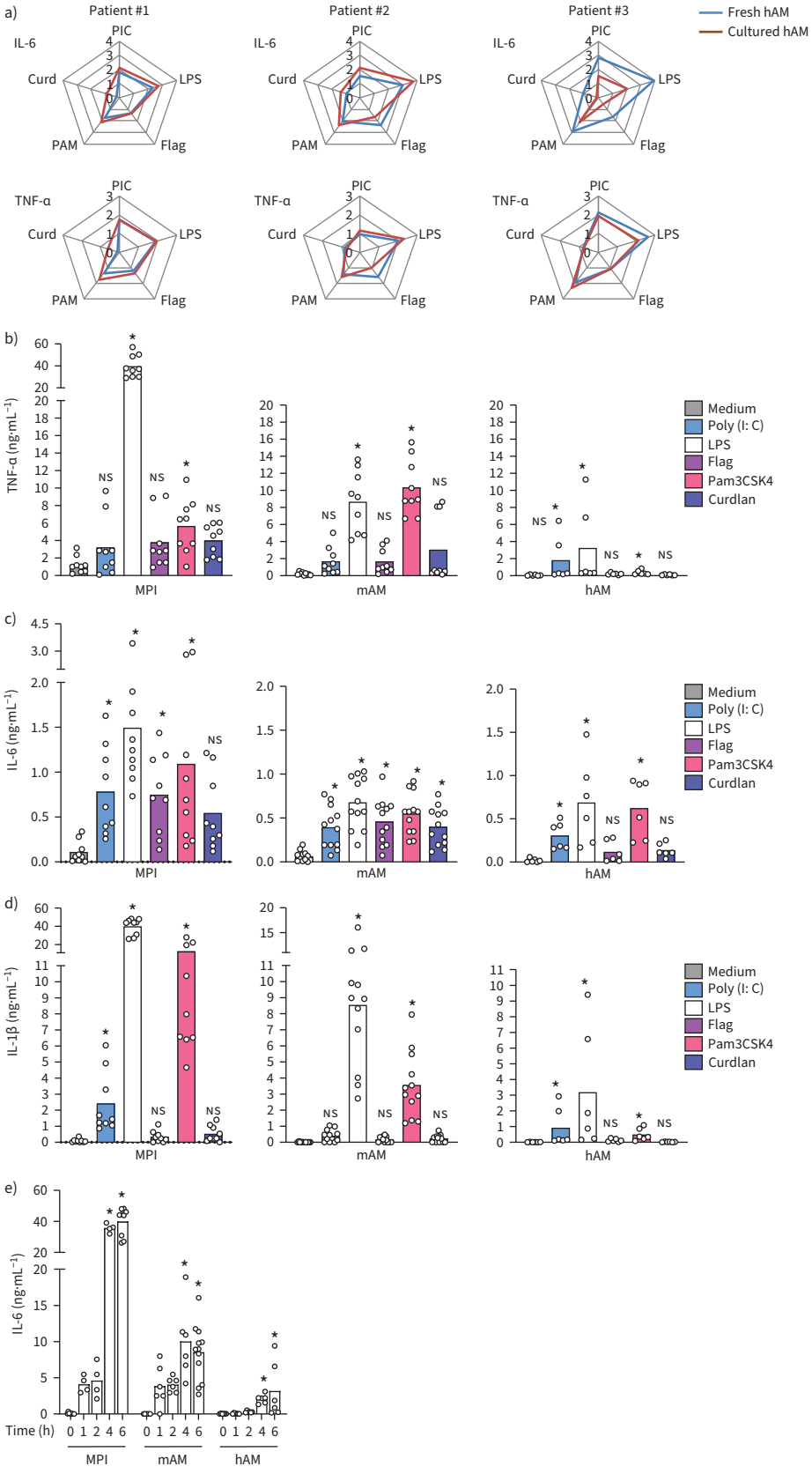

FIGURE 2 Immune responses of murine and human macrophage models to pro-inflammatory agonists. a) Fresh and cultured human alveolar macrophages (hAM) from three donors (patients #1–3) were collected by

bronchoalveolar lavage (BAL), isolated and cultured *ex vivo*. Quantification by ELISA of tumour necrosis factor-α (TNF-α) and interleukin (IL)-6 in the supernatants of fresh hAM (freshly isolated from human bronchoalveolar lavage (hBALF), blue line) compared to cultured hAM (10 days of culture, red line) stimulated for 6 h or not with 20 μg·mL^{-1} of Poly (I: C), 0.1 μg·mL^{-1} of lipopolysaccharide (LPS) from *E. coli* O55:B5, 0.4 μg·mL^{-1} of a recombinant flagellin, 1 μg·mL^{-1} of Pam3CSK4 or 20 μg·mL^{-1} curdlan. b–d) Quantification by ELISA of TNF-α, IL-6 and IL-1β in the supernatants of MPI ("Max Planck Institute cells"), murine AM (mAM) and hAM stimulated for 6 h or not with the same Toll-like receptors (TLRs) in a. e) Quantification by ELISA of IL-6 in the supernatants of MPI, mAM and hAM stimulated for 0, 1, 2, 4 and 6 h with 0.1 μg·mL^{-1} of LPS from *E. coli* O55:B5. a) Data are represented for three donors (referred to as patient #), one to two technical replicates by stimulation condition. Results are expressed in fold changes compared to baseline (in log scale). b) Experiments were replicated as follows: MPI (n=3, three technical replicates), mAM (n=4, three technical replicates, except for IL-6 (n=3, three technical replicates)), hAM (n=3, one to two technical replicates). c) Experiments were replicated as follow: MPI (n=2, two technical replicates, except for at 0 and 6 h (n=3, three technical replicates)), mAM (n=2, three biological replicates, except for at 0 and 6 h (n=4, three technical replicates)), hAM (n=3, two technical replicates). Data are mean and individual values. Statistical analysis was performed using Kruskal–Wallis with Dunn's post-test. NS: non-significance. *p<0.05.

Hence, responses to programmed cell death triggers exhibited notable differences between murine and human AM models, with MPI showing the most significant divergence.

Economic and ecological considerations in experimental model selection

The COVID-19 and ecological crises have highlighted that our resources are not unlimited, emphasising the importance of minimising unnecessary actions and associated waste across all fields, including biological research. We believe that a thorough comparison of experimental models remains incomplete without considering the associated costs and ecological implications.

Assessing the ecological and economic consequences is complex due to ecosystem interconnections and the potential for unforeseen impacts. While acknowledging that our analysis may not be fully exhaustive, we collected verifiable information to quantify the ecological (*i.e.* CO_2 emission and energy consumption in kilowatt-hours) and economic costs (in euros for principal discriminated products) associated with each experimental strategy. This evaluation spanned a defined time horizon, depending on the culture system, to generate 6.10^6 cells needed for experiments depicted in figure 2, repeated three times for all AM models.

Regarding the ecological cost, we found that the total CO_2 emission (CO_2eq) for culturing mAM was seven times higher than for MPI. The main contributing factor was the cell incubator, accounting for 60.4 kg CO_2eq and 8.5 kg CO_2eq respectively for mAM and MPI (table 2). The total plastic waste generated for mAM production was nearly six times higher than that for the same quantity of MPI. CO_2eq for culturing hAM fell in between mAM and MPI (28.6 kg CO_2eq). For comparisons, generating 6.10^6 mAM (emission of 60.4 kg CO_2eq) is roughly equivalent to producing two pairs of jeans, or consuming ∼5–6 kg (11–13 lbs) of beef), or the carbon footprint of a short-haul flight covering ∼156 miles (250 km) per passenger [27].

Regarding the financial cost, the results are in line with the ecological impact, with energy spent for the cell incubator being the primary source of expense. The cost of generating mAM was ∼10 times higher than that of MPI and two times higher than that of hAM (table 2). In summary, each model presents advantages and limitations, influenced by different features illustrated and listed in supplementary figure S3.

Discussion

A man is not a mouse, and *vice versa*. There are clearly numerous interspecies differences, and the intention here was not to create a binary opposition between AM models: human models are obviously more relevant. The aim was to echo G. Box's words, "All models are wrong, but some are useful" [28] and to elucidate what we can learn from murine-derived models in the specific field of AMs and what we cannot. In this study, we present a comparative analysis of AM culture models from mice and humans. Our main observations can be summarised as followed: 1) isolated AMs from mice and humans can be cultured for several days (human) or months (mice); 2) MPI is a self-replicative macrophage model that is easy to culture but lacks typical AM surface marker expression (*i.e.* SiglecF) and presents a more pro-inflammatory phenotype in all tested challenges; 3) responses to TLR agonists are consistent between murine and human AM models, but differences in magnitude should be considered; 4) phagocytic activity of MPI, mAM and cultured hAM were similar; 5) important differences were observed between murine

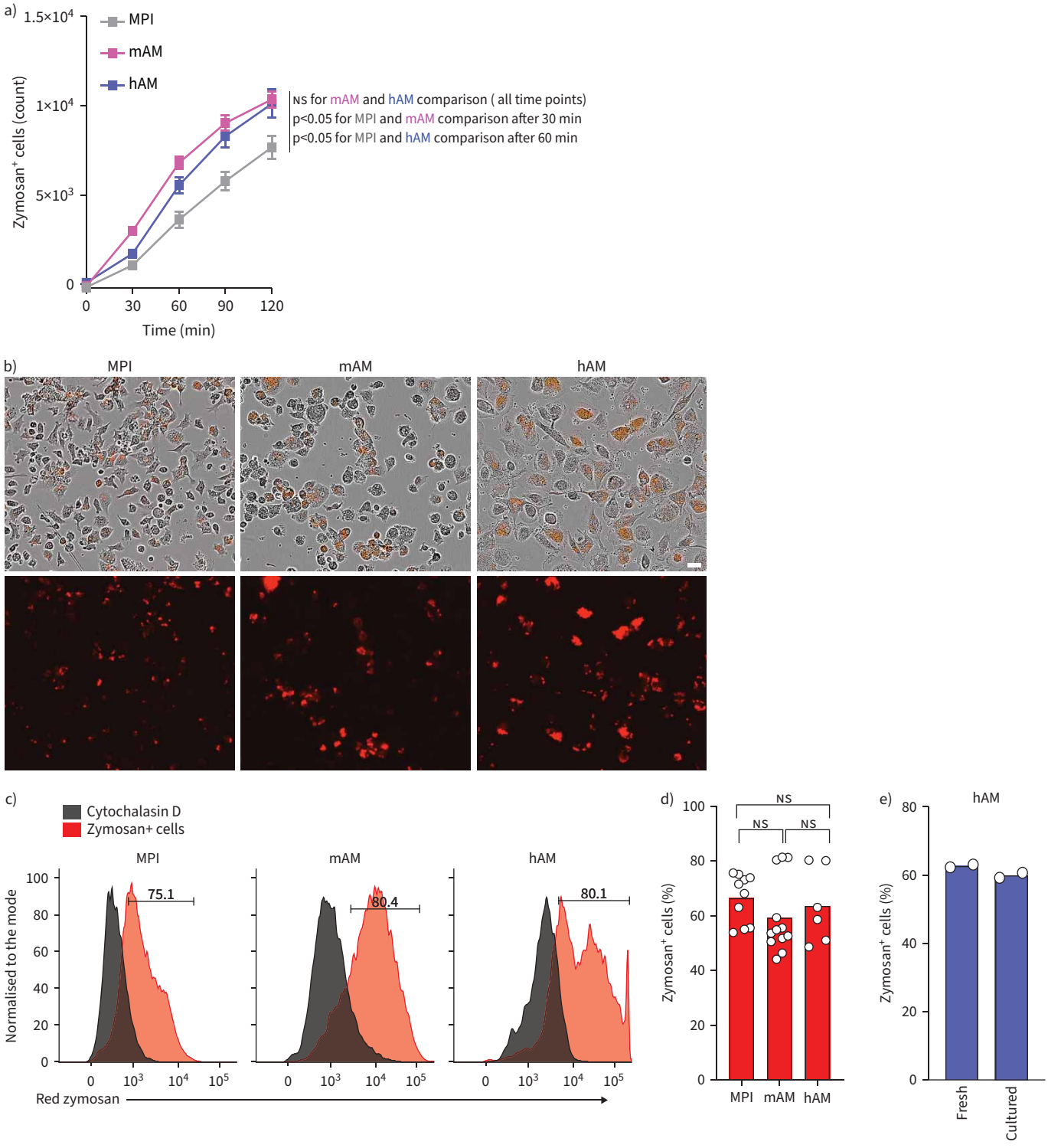

FIGURE 3 MPI ("Max Planck Institute cells"), murine alveolar macrophages (mAM) and human AM (hAM) are capable of efficiently phagocytosing bioparticles. a) Measurement of the phagocytic cells (positive for zymosan and measured using a two-colour IncuCyte SX5 cell-live analysis system of zymosan intake) over time (total duration of 2 h with assessment every 30 min). Each line represents the counts of positive cells, indicated as red cells in b. Cytochalasin D was used as a negative control and to subtract the count of background noise for each point. b) Micrographs showing cells containing red zymosan staining 2 h after exposure. Scale bars: 25 µm. c) Representative plots of positive cells for zymosan (phycoerythrin fluorescence), analysed by flow cytometry 6 h after exposure. Cytochalasin D was used as a negative control to fix the positive labeling threshold. d, e) Percentage of positive cells for zymosan (phycoerythrin fluorescence). Experiments were replicated in parts a and b as follows: MPI (n=2, duplicate), mAM (n=3, triplicate) and hAM (n=3, one to two technical replicates). Experiments were replicated in parts c and d as follows: MPI (n=4,

two to three technical replicates), mAM (n=5, two to three technical replicates) and hAM (n=4, one to two technical replicates). e) Graph represents one donor for fresh hAM and cultured hAM (two technical replicates). a) Data are mean±SEM. Statistical analysis was performed using a two-way RM ANOVA with Tukey's multiple comparisons test. d) Data are mean and individual values. Statistical analysis was performed using Kruskal–Wallis with Dunn's multiple comparisons post-test. NS: non-significant.

and human AMs regarding programmed cell death (apoptosis and pyroptosis), especially for MPI; and 6) ecological and ethical consequences of these AM models are different and sometimes opposed, and should be carefully assessed.

AMs, originating from fetal liver monocytes attracted to the lungs *via* epithelial production of GM-CSF, have been a subject of extensive investigation. Early efforts focused on culturing fetal liver cells with GM-CSF, yielding self-replicating AM-like cells termed MPI. MPI offer distinct advantages in terms of culture simplicity, cost-effectiveness and ethical considerations, making them widely utilised in collaborative and comparative research endeavours (supplementary figure S3). However, a notable drawback is the gradual loss of typical AM surface markers (CD11c and SiglecF) over time, a phenomenon also observed by others [10, 29]. The implications of these alterations, particularly in the context of MPI's pro-inflammatory phenotype compared to primary cultured AMs, remain uncertain. SiglecF, implicated in regulating inflammatory responses by potentially mitigating inflammation and aiding immune response resolution in the lungs [30, 31], may play a pivotal role due to its immunoreceptor tyrosine-based inhibitory motifs (ITIMs) interacting with immunoreceptor tyrosine-based activation motifs (ITAMs) [32, 33]. The decline in SiglecF expression could contribute to MPI's pro-inflammatory profile. To maintain an AM-like phenotype, some have proposed culturing fetal liver-derived cells with transforming growth factor-β (TGF-β) alongside GM-CSF, which preserved high SiglecF expression levels [29]. However, we opted against adding TGF-β to our MPI culture for several reasons. Firstly, introducing TGF-β post-initial culture would not revert MPI to an AM phenotype. Secondly, incorporating TGF-β would hinder direct comparisons with other AM models or necessitate its inclusion across all conditions. Lastly, considering that we can now obtain and culture AMs directly from lungs, it raises questions about whether we still need to derive cells from the liver.

We have established that mAM can be sustained in long-term culture, undergoing extensive expansion while retaining their tissue-resident identity intact. This provides a substantial supply of genetically unaltered and untransformed macrophages, significantly reducing the need for animal sacrifice. Unlike traditional cell lines, mAM cultures offer the convenience of a continuous cell source without the need for complex differentiation protocols or concerns about genetic modifications or distant origins. Furthermore, this long-term culture system allows for seamless transitions between *in vitro* and *in vivo* environments, maintaining cellular identity consistently. This presents exciting potential for direct *in vivo* validation of experimental findings. Although we observed minor adaptations in surface marker expression of mAM in the culture environment (see figure 1), crucial AM-specific markers such as SiglecF and CD11c remained stable throughout prolonged culture periods (6–7 months), even through freeze–thaw cycles, affirming their robust AM-specific identity. Additionally, recent evidence indicates that these minor alterations are entirely reversible upon transplantation into the alveolar niche [9]. The establishment of robust long-term mAM cultures represents a significant advancement in biological research, accelerating our understanding of AM pathophysiology. However, until now, the translational potential of mAM cultures to human studies remained uncertain. Our study addresses this gap by demonstrating that, despite some disparities, mAM exhibit high translational relevance in terms of inflammatory responses and phagocytosis. Conversely, differences in cell death pathways between murine and human AMs were evident. These differences may be attributed to variations in the balance of specific caspase proteins, as documented in studies of lymphocyte death pathways [34–36]. Indeed, mice lack caspase 10 and the deletion of caspase 8 is embryonic lethal, whereas lack of caspase 8 in humans induces immunodeficiencies [34, 36].

Despite their considerable promise, mAM encounter several limitations that merit consideration. Firstly, under normal conditions, the majority of AMs are considered sessile cells, adhering to the epithelium [37]. Hence, lavage-isolated primary AMs may not fully represent the entire AM pool, potentially overlooking those firmly attached to the epithelium [38]. While collecting AM lung digest could mitigate this issue, it introduces challenges such as potential alterations to cell phenotype due to sorting techniques and the complexity of isolation procedures. Secondly, the absence of a three-dimensional setting in *ex vivo* primary cell cultures may limit the exploration of AM physiopathology. Indeed, AM physiopathology is extremely sensitive to cell-to-cell interactions and other components of the alveolar niche. Consequently, alternative 3D *ex vivo* systems, such as multicellular lung organoids or precision-cut lung slices, offer promising

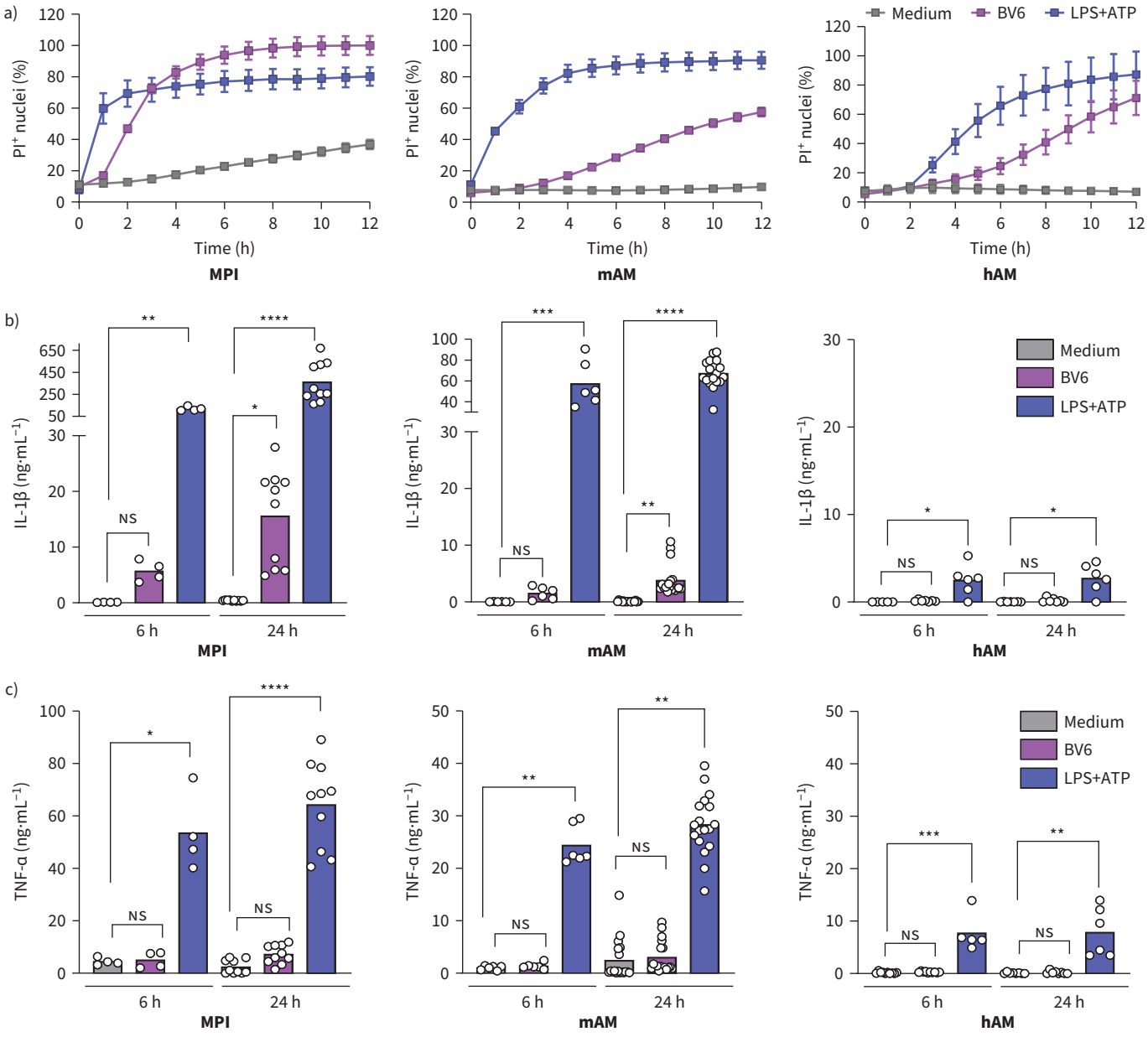

FIGURE 4 Murine alveolar macrophage (mAM) models showing differences in programmed cell deaths compared to human AM (hAM). a) Dead cell counts over time after BV6 (20 µm) or lipopolysaccharide (LPS; 100 ng·mL^{-1})+ATP (5 mM) treatments. PI: propidium iodide. Quantification by ELISA of b) interleukin (IL)-1β and c) tumour necrosis factor-α (TNF-α) levels in the supernatants of MPI ("Max Planck Institute cells"), mAM and hAM stimulated or not for 6 h and 24 h. Experiments were replicated as follows: MPI (n=2–4, two to three technical replicates), mAM (n=3–7, two to three technical replicates), hAM (n=3, two technical replicates). a) Data are mean±SEM. b and c) Data are mean and individual values. Statistical analysis was performed using Kruskal–Wallis with Dunn's post-test. NS: non-significant. *p<0.05, **p<0.005, ***p<0.0005, ****p<0.0001.

avenues despite their technical and organisational complexities. Thirdly, our comparison involves AMs isolated from young naive mice and human adults. Ageing significantly impacts immune cell function, with observed age-related changes in monocytes and macrophages [39, 40]. Matching ages proves difficult due to the infrequent performance of BAL procedures on young humans, and aged mice are notably more expensive and less accessible. Finally, AMs are known to be remodelled after infectious challenges [11, 41]. AM changes likely contribute to the improved defence against respiratory infection. This process has been termed "trained immunity" and defines activation of the innate immune system that results in enhanced responsiveness to subsequent triggers [42]. Human adults have experienced lung infections and exposures that may have impacted their capacity to fight novel infections, while, in contrast, experimental mice are housed in controlled atmospheres and have not or poorly experienced trained immunity. Our prior

examination of the relevance of murine AMs to humans, particularly in the context of prior lung infection history, revealed that transcriptome data from AMs of mice become even more similar to humans following respiratory infections [11]. Thus, culturing AMs from mice with trained immunity *ex vivo* could represent a significant advancement.

As far as we know, we are pioneering the inclusion of ecological examination in cell models generation. We anticipate that such analyses, especially concerning ecological costs, may emerge as a pivotal element in shaping future scientific considerations.

This study has further limitations. First, gating strategies often lead to discussion on AMs. Here, we selected surface markers and gating strategy based on previous studies that highlighted the better combinations to discriminate the population of AMs [1, 15, 43]. In humans, CD169, combined with HLA-DR, CD11b and CD206, appears to be the most discriminative for AMs among the lung macrophage populations [43]. Interspecies similarities and differences have been taken into account [5]. Second, the culturing conditions may also raise debate. Despite some evidence for using GM-CSF and TGF-β for maintaining the AM phenotype, we chose to use GM-CSF alone for the maintenance of mouse and human AMs during culture, because the recent work from Subramamian *et al.* [9] demonstrated that the use of GM-CSF is sufficient to maintain long-term proliferation of cultured mAM without compromising cellular identity *in vivo*. We acknowledge that there is no consensus on this matter. We did not used a cocktail of lung-associated components for long-term hAM culture because the purpose was to use hAM shortly after sampling. Third, patients of our study cannot be considered as normal healthy donors because the mean age was 67 years, and nearly half of them were former or active smokers. However, they are representative of a real-life setting; the one we want to model. Fourth, we highlight the varying responses to programmed cell death among the different macrophage models. However, we did not study the underlying mechanisms because it was outside the scope of our work. Finally, it seems nearly impossible to achieve a complete costs and ecological assessment. We acknowledge that our evaluation can be improved on. However, as far as we know, we are pioneering the inclusion of ecological examination in cell model generation. We anticipate that such analyses, especially concerning ecological costs, may emerge as a pivotal element in shaping future scientific considerations.

In conclusion, the progress of biological research has been significantly shaped by the substantial impact of cell culture. The use of murine *ex vivo* cultured AMs holds promise for advancing our research and reducing dependence on mouse *in vivo* experimentation. However, it is essential to determine the mice-to-human translational values of experimental observations in these cell models. With this proof-of-principle that hAM can be cultured and studied *ex vivo*, the authors acknowledge that whenever it is possible, human AMs should be used as they will certainly better recapitulate overall human immune response.

Acknowledgements: We acknowledge all healthcare coworkers involved in the pulmonary department at the Bretonneau Hospital for their excellent management of patient samples. We thank Sandrine Henri (INSERM, Centre d'Etude des Pathologies Respiratoires (CEPR), UMR 1100, Tours, France) for the reviewing of the manuscript.

Provenance: Submitted article, peer reviewed.

Ethics statement: Study of human samples was approved by the IRB of the Tours University Hospital (Espace de Réflexion Éthique de la Région Centre) and the human sample collection was reported to the competent authority (Ministère Français de l'Enseignement Supérieur, de la Recherche et de l'Innovation, DC-2014-2285). Informed consent was obtained from all subjects. The study was conformed to the principles set out in the VMA Declaration of Helsinki and the Department of Health and Human Service Belmont Report. C57Bl/6 male and female mice were purchased from the Centre d'Elevage R. Janvier (Le Genest Saint-Isle, France) and were used at about 8–10 weeks of age. Mice were treated in accordance with the European animal welfare regulation. Mice were bred in an animal facility in pathogen-free conditions. All animal experimentations were performed according to the ethical guidelines and were approved by our local and national ethics committee (CEEA.19, #201604071220401-4885).

Author contributions: C. David: conceptualisation, investigation, methodology, formal analysis, validation, visualisation and writing (original draft, review and editing). D. Brea, A. Cezard, V. Vasseur, C. Verney, S. Khau and E. Barsac: investigation, methodology, validation, review and editing. B. Briard: formal analysis, review and editing. M. Ferreira and S. Marchand-Adam: methodology, formal analysis, review and editing. M. Si-Tahar and A. Guillon: conceptualisation, formal analysis, supervision, validation, visualisation and writing (original draft, review and editing). A. Cezard: drawing of supplementary figure S3.

Conflict of interest: No competing interests to declare.

Support statement: The study was supported by the Agence Nationale de la Recherche (ANR-23-CE14-0057 (FLUMACRO)). Funding information for this article has been deposited with the Crossref Funder Registry.

References

1 Yu Y-RA, Hotten DF, Malakhau Y, *et al.* Flow cytometric analysis of myeloid cells in human blood, bronchoalveolar lavage, and lung tissues. *Am J Respir Cell Mol Biol* 2016; 54: 13–24.
2 Busch CJ-L, Favret J, Geirsdóttir L, *et al.* Isolation and long-term cultivation of mouse alveolar macrophages. *Bio Protoc* 2019; 9: e3302.
3 Aegerter H, Lambrecht BN, Jakubzick CV. Biology of lung macrophages in health and disease. *Immunity* 2022; 55: 1564–1580.
4 Murray PJ, Allen JE, Biswas SK, *et al.* Macrophage activation and polarization: nomenclature and experimental guidelines. *Immunity* 2014; 41: 14–20.
5 Bain CC, MacDonald AS. The impact of the lung environment on macrophage development, activation and function: diversity in the face of adversity. *Mucosal Immunol* 2022; 15: 223–234.
6 Nahrendorf M, Swirski FK. Abandoning M1/M2 for a network model of macrophage function. *Circ Res* 2016; 119: 414–417.
7 Fejer G, Wegner MD, György I, *et al.* Nontransformed, GM-CSF–dependent macrophage lines are a unique model to study tissue macrophage functions. *Proc Natl Acad Sci USA* 2013; 110: E2191–E2198.
8 Pernet E, Sun S, Sarden N, *et al.* Neonatal imprinting of alveolar macrophages via neutrophil-derived 12-HETE. *Nature* 2023; 614: 530–538.
9 Subramanian S, Busch CJ-L, Molawi K, *et al.* Long-term culture-expanded alveolar macrophages restore their full epigenetic identity after transfer in vivo. *Nat Immunol* 2022; 23: 458–468.
10 Gorki A-D, Symmank D, Zahalka S, *et al.* Murine ex vivo cultured alveolar macrophages provide a novel tool to study tissue-resident macrophage behavior and function. *Am J Respir Cell Mol Biol* 2022; 66: 64–75.
11 Guillon A, Arafa EI, Barker KA, *et al.* Pneumonia recovery reprograms the alveolar macrophage pool. *JCI Insight* 2020; 5: e133042.
12 Correa-Macedo W, Fava VM, Orlova M, *et al.* Alveolar macrophages from persons living with HIV show impaired epigenetic response to *Mycobacterium tuberculosis*. *J Clin Invest* 2021; 131: e148013.
13 Kamel T, Helms J, Janssen-Langenstein R, *et al.* Benefit-to-risk balance of bronchoalveolar lavage in the critically ill. A prospective, multicenter cohort study. *Intensive Care Med* 2020; 46: 463–474.
14 Mankikian J, Ehrmann S, Guilleminault L, *et al.* An evaluation of a new single-use flexible bronchoscope with a large suction channel: reliability of bronchoalveolar lavage in ventilated piglets and initial clinical experience. *Anaesthesia* 2014; 69: 701–706.
15 Bharat A, Bhorade SM, Morales-Nebreda L, *et al.* Flow cytometry reveals similarities between lung macrophages in humans and mice. *Am J Respir Cell Mol Biol* 2016; 54: 147–149.
16 O'Neill LAJ, Pearce EJ. Immunometabolism governs dendritic cell and macrophage function. *J Exp Med* 2016; 213: 15–23.
17 Kelly B, O'Neill LA. Metabolic reprogramming in macrophages and dendritic cells in innate immunity. *Cell Res* 2015; 25: 771–784.
18 Lukashev D, Ohta A, Apasov S, *et al.* Cutting edge: physiologic attenuation of proinflammatory transcription by the Gs protein-coupled A2A adenosine receptor in vivo. *J Immunol* 2004; 173: 21–24.
19 Cezard A, Monard S, Bréa-Diakite D, *et al.* [Metabokines reviewed: essential mediators of anti-infectious immunity]. *Med Sci (Paris)* 2021; 37: 342–348.
20 Guillon A, Brea-Diakite D, Cezard A, *et al.* Host succinate inhibits influenza virus infection through succinylation and nuclear retention of the viral nucleoprotein. *EMBO J* 2022; 41: e108306.
21 Tannahill GM, Curtis AM, Adamik J, *et al.* Succinate is an inflammatory signal that induces IL-1β through HIF-1α. *Nature* 2013; 496: 238–242.
22 Mills EL, Kelly B, Logan A, *et al.* Succinate dehydrogenase supports metabolic repurposing of mitochondria to drive inflammatory macrophages. *Cell* 2016; 167: 457–470.e13.
23 Häcker G. Apoptosis in infection. *Microbes Infect* 2018; 20: 552–559.
24 Brokatzky D, Mostowy S. Pyroptosis in host defence against bacterial infection. *Dis Model Mech* 2022; 15: dmm049414.
25 Gurung P, Li B, Subbarao Malireddi RK, *et al.* Chronic TLR stimulation controls NLRP3 inflammasome activation through IL-10 mediated regulation of NLRP3 expression and caspase-8 activation. *Sci Rep* 2015; 5: 14488.
26 Varfolomeev E, Blankenship JW, Wayson SM, *et al.* IAP antagonists induce autoubiquitination of C-IAPs, NF-κB activation, and TNFα-dependent apoptosis. *Cell* 2007; 131: 669–681.
27 Ritchie H, Roser M. Which form of transport has the smallest carbon footprint? *Our World in Data.* Date last updated: 30 August 2023. https://ourworldindata.org/travel-carbon-footprint
28 Box GEP. Science and Statistics. *J Am Stat Assoc* 1976; 71: 791–799.
29 Thomas ST, Wierenga KA, Pestka JJ, *et al.* Fetal liver–derived alveolar-like macrophages: a self-replicating ex vivo model of alveolar macrophages for functional genetic studies. *ImmunoHorizons* 2022; 6: 156–169.

30 Kiwamoto T, Katoh T, Tiemeyer M, *et al.* The role of lung epithelial ligands for Siglec-8 and Siglec-F in eosinophilic inflammation. *Curr Opin Allergy Clin Immunol* 2013; 13: 106–111.
31 Patnode ML, Cheng C-W, Chou C-C, *et al.* Galactose 6-O-sulfotransferases are not required for the generation of Siglec-F ligands in leukocytes or lung tissue. *J Biol Chem* 2013; 288: 26533–26545.
32 Feng Y, Mao H. Expression and preliminary functional analysis of Siglec-F on mouse macrophages. *J Zhejiang Univ Sci B* 2012; 13: 386–394.
33 Crocker PR, Paulson JC, Varki A. Siglecs and their roles in the immune system. *Nat Rev Immunol* 2007; 7: 255–266.
34 Mestas J, Hughes CCW. Of mice and not men: differences between mouse and human immunology. *J Immunol* 2004; 172: 2731–2738.
35 Tibbetts MD, Zheng L, Lenardo MJ. The death effector domain protein family: regulators of cellular homeostasis. *Nat Immunol* 2003; 4: 404–409.
36 Chun HJ, Zheng L, Ahmad M, *et al.* Pleiotropic defects in lymphocyte activation caused by caspase-8 mutations lead to human immunodeficiency. *Nature* 2002; 419: 395–399.
37 Westphalen K, Gusarova GA, Islam MN, *et al.* Sessile alveolar macrophages communicate with alveolar epithelium to modulate immunity. *Nature* 2014; 506: 503–506.
38 Bhattacharya J, Westphalen K. Macrophage-epithelial interactions in pulmonary alveoli. *Semin Immunopathol* 2016; 38: 461–469.
39 Ray D, Yung R. Immune senescence, epigenetics and autoimmunity. *Clin Immunol* 2018; 196: 59–63.
40 Wong CK, Smith CA, Sakamoto K, *et al.* Aging impairs alveolar macrophage phagocytosis and increases influenza-induced mortality in mice. *J Immunol 1950* 2017; 199: 1060–1068.
41 Arafa EI, Shenoy AT, Barker KA, *et al.* Recruitment and training of alveolar macrophages after pneumococcal pneumonia. *JCI Insight* 2022; 7: e150239.
42 Netea MG, Domínguez-Andrés J, Barreiro LB, *et al.* Defining trained immunity and its role in health and disease. *Nat Rev Immunol* 2020; 20: 375–388.
43 Morrell ED, Wiedeman A, Long SA, *et al.* Cytometry TOF identifies alveolar macrophage subtypes in acute respiratory distress syndrome. *JCI Insight* 2018; 3: e99281.